Supplementary Information for: Rapid and Accurate Determination of Nanopore Ionic Current Using a Steric Exclusion Model

James Wilson*,† Kumar Sarthak*,‡ Wei Si,¶,† Luyu Gao,† and Aleksei Aksimentiev*,†,§

†*Department of Physics, University of Illinois at Urbana-Champaign, Urbana, Illinois 61801, United States*

‡*Center for Biophysics and Quantitative Biology, University of Illinois at Urbana-Champaign, Urbana, Illinois 61801, United States*

¶ *Jiangsu Key Laboratory for Design and Manufacture of Micro-Nano Biomedical Instruments and School of Mechanical Engineering, Southeast University, Nanjing, 210096, China*

§*Beckman Institute for Advanced Science and Technology, University of Illinois at Urbana-Champaign, Urbana, Illinois 61801, United States*

* These authors contributed equally to the manuscript

E-mail: aksiment@illinois.edu

5 Supporting Figures and 1 Supporting Table. Total number of pages: 10.

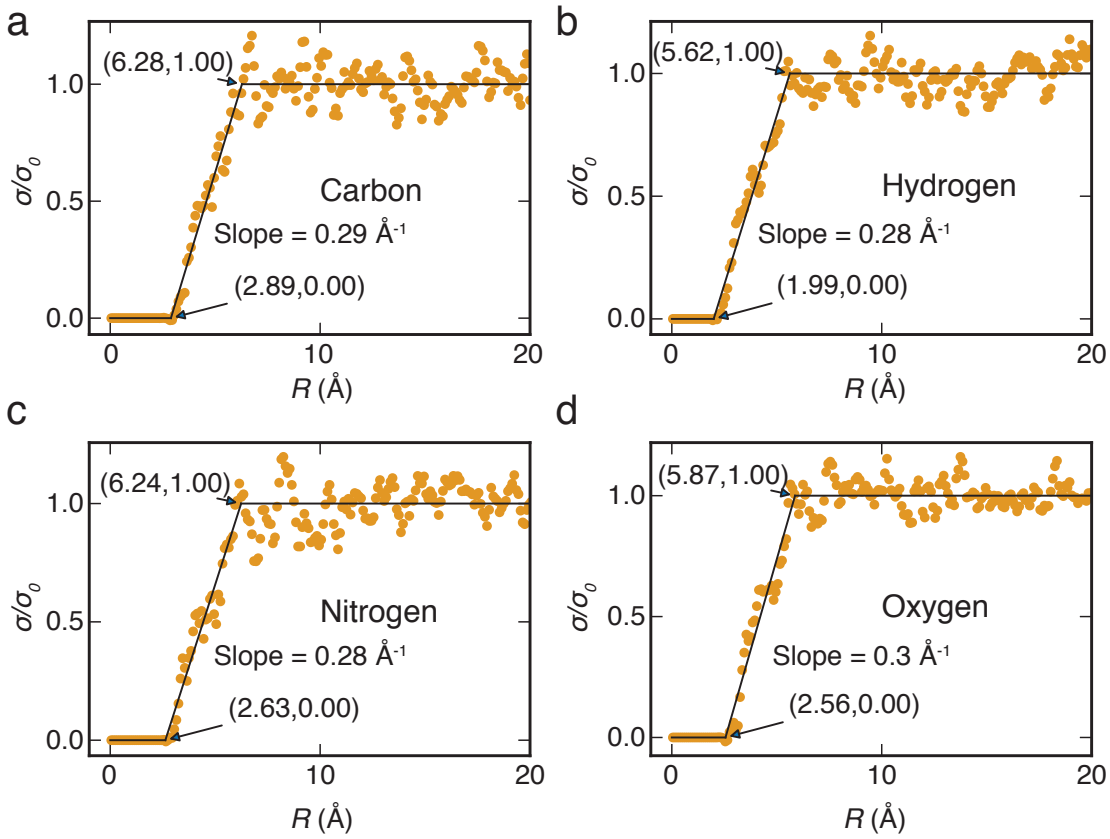

Figure S1: Simulated conductivity σ of KCl electrolyte as a function of distance R from the center of a line of carbon (a), hydrogen (b), nitrogen (c), oxygen (d) atoms, scaled by the bulk conductivity σ_0. The main text Fig. 2a & b show the simulation system. Piecewise linear approximation is shown in black.

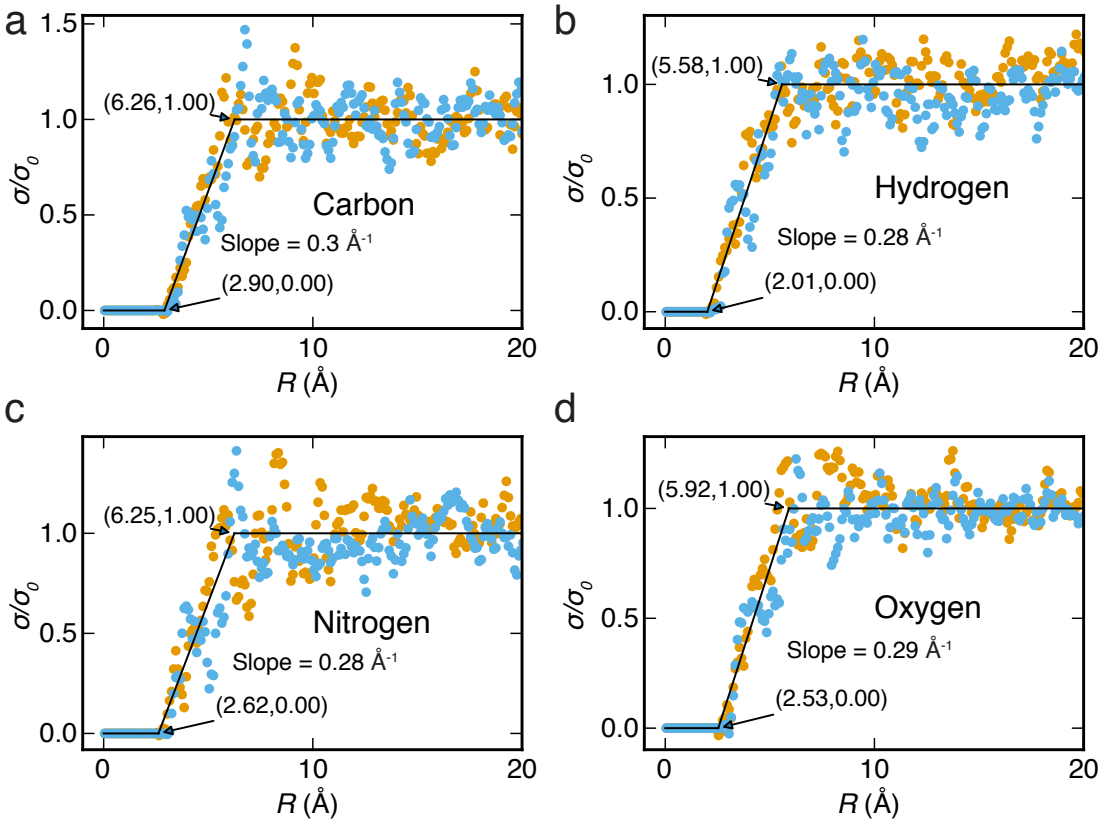

Figure S2: Simulated conductivity σ of K^+ (orange) and Cl^- (blue) species of 1M KCl electrolyte as a function of distance R from the center of a line of carbon (a), hydrogen (b), nitrogen (c), oxygen (d) atoms, scaled by the bulk conductivity σ_0. The main text Fig. 2a & b show the simulation system. Piecewise linear approximation is shown in black.

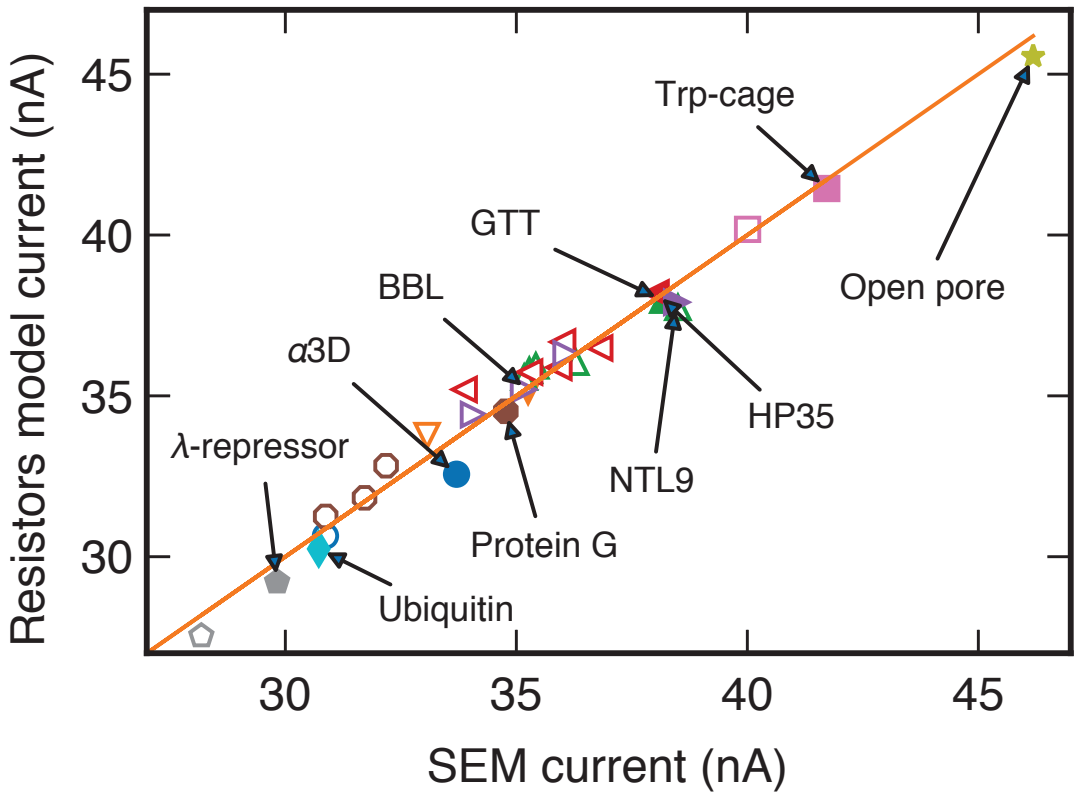

Figure S3: Comparison of the nanopore currents computed using the resistors model described in Ref. 1 against SEM. The simulation system is shown in the main text Fig. 3a. Data for proteins of identical amino acid sequences but different folding states and/or orientations are shown using symbols of the same shape and color. Filled/open symbols correspond to folded/unfolded proteins, respectively. The orange line (of slope 1 and intercept of 0) indicates perfect agreement between the two methods.

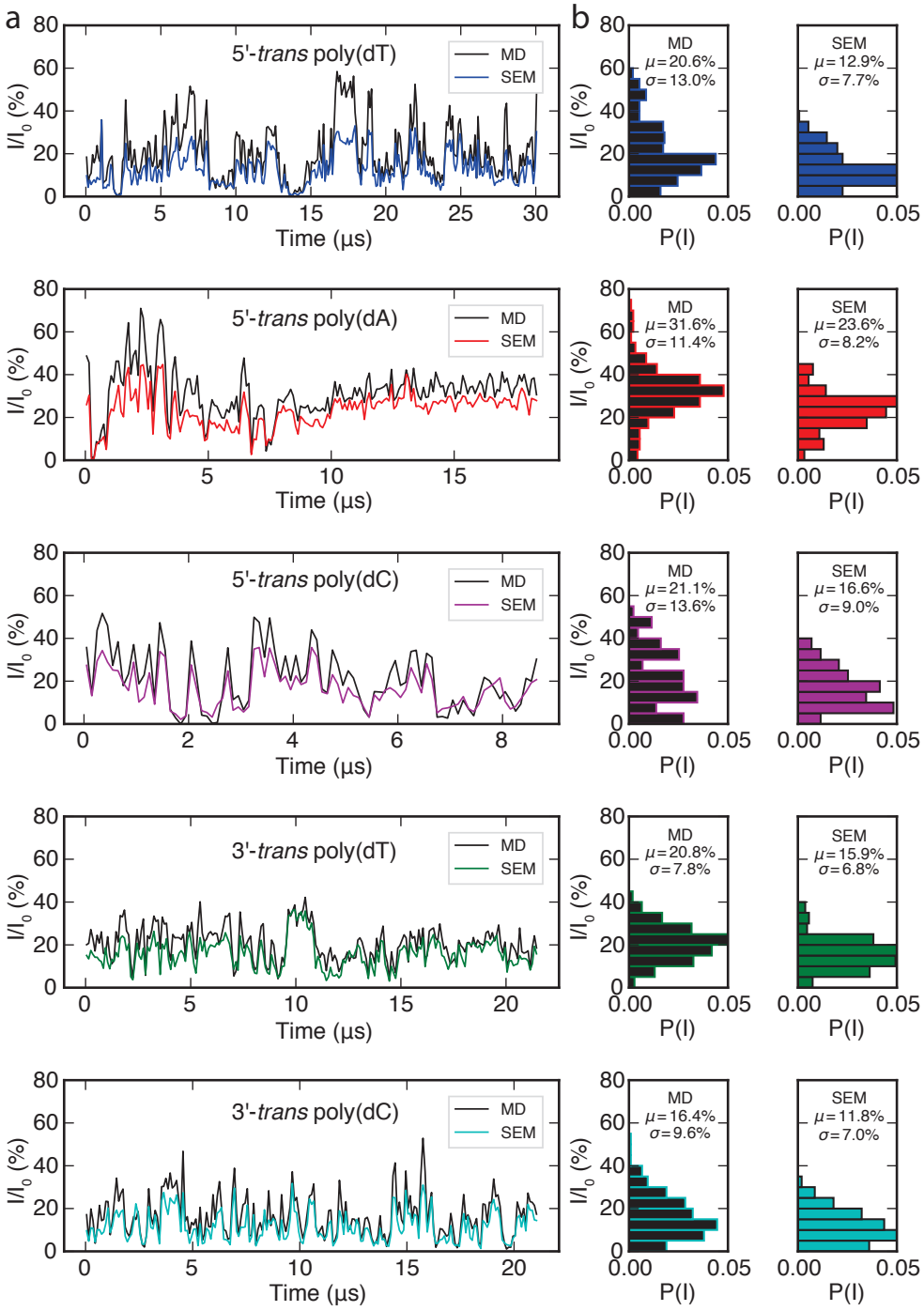

Figure S4: Comparison of the SEM and MD blockade currents in MspA done using nominal bulk conductivity of 1.1 M KCl. (a) Ionic current measured from displacement of ions in explicit solvent MD simulations (black) and computed from the coordinates of DNA and MspA using SEM (colors). For both methods, the transmembrane bias was set to 180 mV, the current was sampled every 100 ps and averaged in 100 ns blocks. (b) Histograms of blockade currents obtained using explicit solvent MD (black) and SEM (colors). Main text Fig. 5a shows typical simulation systems.

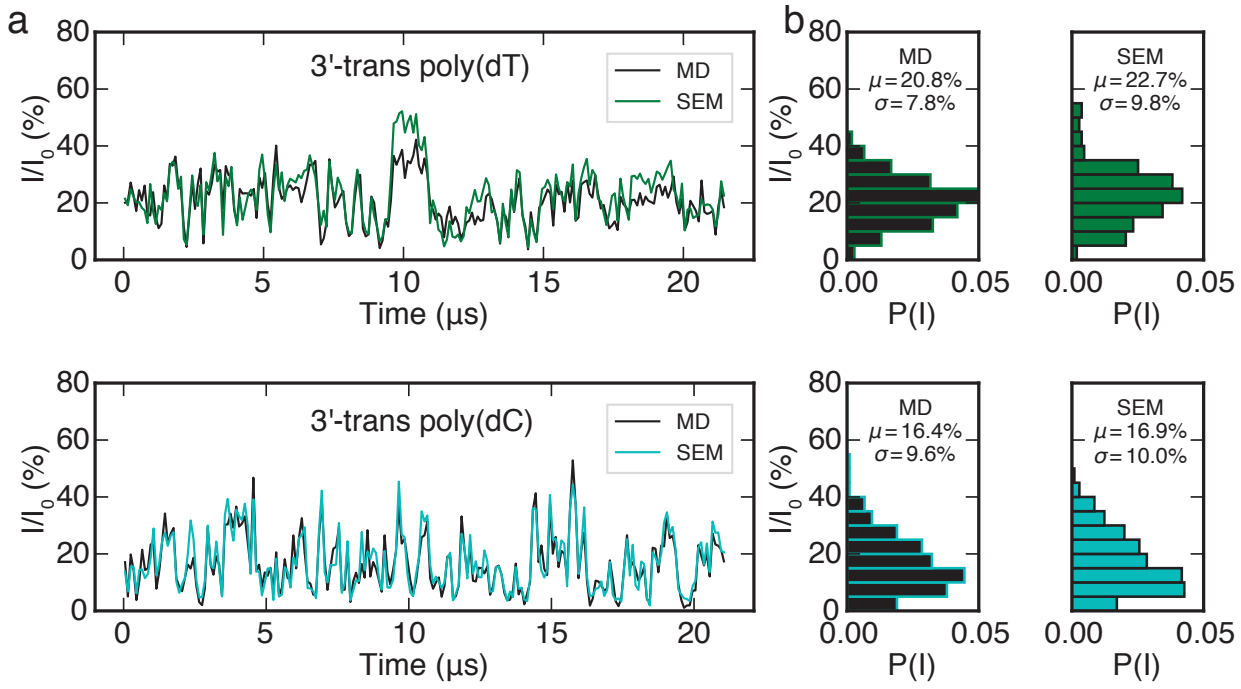

Figure S5: Comparison of the SEM and MD blockade currents for 3′-*trans* DNA homopolymer/MspA systems done using effective bulk conductivity of 1.4 M KCl. (a) Ionic current measured from displacement of ions in explicit solvent MD simulations (black) and computed from the coordinates of DNA and MspA using SEM (colors). For both methods, the transmembrane bias was set to 180 mV, the current was sampled every 100 ps and averaged in 100 ns blocks. (b) Histograms of blockade currents obtained using explicit solvent MD (black) and SEM (colors). Main text Fig. 5a shows typical simulation systems.

Methods for MD simulations of biological nanopores

SI Table S1 summarizes the conditions used for the MD simulations of biological nanopores. Initial atomic models of the biological nanopores were taken from the Protein Data Bank, see PDB ID column of SI Table S1. The model of G20C viral portal protein was obtained by mutating all 49L residues to cysteines; the porphyrin moieties were added via harmonic bonds linking them to the sulphur atoms of C49 residues.[2] The FhuA structure was modified to produce a ΔC/Δ5L deletion mutant as described in our previous work .[3] The MspA structure was adjusted to represent the M1-NNN (D20N/D91N/D93N) mutant; the vestibule of the MspA protein was truncated to retain only residues 75-120, see Ref. 4 for details.

Each system was built by aligning a patch of pre-equilibrated lipid bilayer with the x–y plane. The biological nanopore was oriented to have its symmetry axis aligned with the z axis. The hydrophobic stem of each nanopore was placed at the center of the bilayer and all residues of the bilayer that had an atom in contact with the pore were removed. The protein and lipid system was then solvated in TIP3P water. After neutralizing the net charge of the system, ions were added to make a 1M KCl or NaCl solution. The final dimensions of each system and the total number of atoms are specified in column 3 and 4 of Table S1, respectively. After energy minimization, each system was heated to 295 K. Following that, the systems were equilibrated in an NPT ensemble to attain equilibrium volume. These NPT simulations were carried out maintaining the constant ratio of the systems' dimension in the x–y plane. The equilibrated system was used for ionic current simulations carried out in the NVT ensemble; the systems' dimension were the average values form the NPT equilibration. Constant electric field was applied along the z direction to produce the target transmembrane voltage (column 6, Table S1). The simulations were run for the specified number of nanoseconds; the ionic currents were computed by summing up instantaneous displacements of ions along the MD trajectory.[5]

Table S1: Conditions for MD simulations of biological nanopores. The PDB ID column specifies the initial crystallographic structure before introducing mutations or deletions to represent the experimental nanopore system. The Ions column specify the type of electrolyte used in the MD simulations; the bulk electrolyte concentration was 1 M in all systems. DPhPC lipid bilayer refers to 1,2-diphytanoyl-sn-glycero-3-phosphocholine and POPC lipid bilayer refers to 1-palmitoyl-2-oleoyl-glycero-3-phosphocholine.

Biological nanopore	**PDB ID**	**System size (nm^3)**	**Number of atoms**	**Simulation time**	**Voltage bias**	**Ions**	**Lipid bilayer**
Aerolysin	5JZT[6]	19.2×19.2×14.5	447,121	20 ns	500mV	KCl	DPhPC
G20C	4ZJN[7]	20.4×20.4×18.3	792,643	35 ns	100mV	NaCl	DPhPC
OprD	3SYZ[8]	8.4 × 8.4 × 10.9	81,934	650 ns	80mV	KCl	DPhPC
α-HL	7AHL[9]	14.4×14.4×18.4	391,165	250 ns	120mV	KCl	DPhPC
OmpF	2OMF[10]	12.1 × 12.1 × 7.5	110,608	40 ns	500mV	NaCl	POPC
FhuA	1BY5[11]	12.5×12.5×11.2	184,448	240 ns	-80mV	KCl	DPhPC
ClyA	2WCD[12]	20.0×20.0×21.2	872,479	120 ns	120mV	KCl	DPhPC
FraC	4TSY[13]	14.1×14.1×17.5	357,179	35 ns	1.2V	NaCl	DPhPC
MspA	1UUN[14]	6.6 × 6.6 × 5.5	13,548	500 ns	180mV	KCl	POPC
AQP-1	1J4N[15]	9.3 × 8.6 × 7.7	65,497	150 ns	0V	neutral	POPE

References

1. Si, W.; Aksimentiev, A. Nanopore Sensing of Protein Folding. *ACS Nano* **2017**, *11*, 7091–7100.

2. Cressiot, B.; Greive, S. J.; Si, W.; Pascoa, T.; Mojtabavi, M.; Chechik, M.; Jenkins, H. T.; Lu, X.; Zhang, K.; Aksimentiev, A. *et al.* Porphyrin-Assisted Docking of

a Thermophage Portal Protein into Lipid Bilayers: Nanopore Engineering and Characterization. *ACS Nano* **2017**, *11*, 11931–11945.

3. Wolfe, A. J.; Si, W.; Zhang, Z.; Blanden, A. R.; Hsueh, Y.-C.; Gugel, J. F.; Pham, B.; Chen, M.; Loh, S. N.; Rozovsky, S. *et al.* Quantification of Membrane Protein-Detergent Complex Interactions. *J. Phys. Chem. B* **2017**, *121*, 10228–10241.

4. Bhattacharya, S.; Yoo, J.; Aksimentiev, A. Water Mediates Recognition of DNA Sequence *via* Ionic Current Blockade in a Biological Nanopore. *ACS Nano* **2016**, *10*, 4644–4651.

5. Aksimentiev, A.; Schulten, K. Imaging α-Hemolysin with Molecular Dynamics: Ionic Conductance, Osmotic Permeability and the Electrostatic Potential Map. *Biophys. J.* **2005**, *88*, 3745–3761.

6. Iacovache, I.; Carlo, S. D.; Cirauqui, N.; Peraro, M. D.; Goot, F. G. V. D.; Zuber, B. Cryo-EM structure of aerolysin variants reveals a novel protein fold and the pore-formation process. *Nat. Commun.* **2016**, *7*.

7. Williams, L. S.; Levdikov, V. M.; Minakhin, L.; Severinov, K.; Antson, A. A. 12-Fold symmetry of the putative portal protein from the Thermus thermophilus bacteriophage G20C determined by X-ray analysis. *Acta Cryst. F* **2013**, *69*, 1239–1241.

8. Eren, E.; Vijayaraghavan, J.; Liu, J.; Cheneke, B. R.; Touw, D. S.; Lepore, B. W.; Indic, M.; Movileanu, L.; Van den Berg, B. Substrate specificity within a family of outer membrane carboxylate channels. *PLoS Biol.* **2012**, *10*, e1001242.

9. Song, L.; Hobaugh, M. R.; Shustak, C.; Cheley, S.; Bayley, H.; Gouaux, J. E. Structure of staphylococcal α-hemolysin, a heptameric transmembrane pore. *Science* **1996**, *274*, 1859–1865.

10. Cowan, S.; Schirmer, T.; Rummel, G.; Steiert, M.; Ghosh, R.; Pauptit, R.; Jansonius, J.; Rosenbusch, J. Crystal structures explain functional properties of two E. coli porins. *Nature* **1992**, *358*, 727.

11. Locher, K. P.; Rees, B.; Koebnik, R.; Mitschler, A.; Moulinier, L.; Rosenbusch, J. P.; Moras, D. Transmembrane signaling across the ligand-gated FhuA receptor: crystal structures of free and ferrichrome-bound states reveal allosteric changes. *Cell* **1998**, *95*, 771–778.

12. Mueller, M.; Grauschopf, U.; Maier, T.; Glockshuber, R.; Ban, N. The structure of a cytolytic α-helical toxin pore reveals its assembly mechanism. *Nature* **2009**, *459*, 726.

13. Tanaka, K.; Caaveiro, J. M.; Morante, K.; González-Mañas, J. M.; Tsumoto, K. Structural basis for self-assembly of a cytolytic pore lined by protein and lipid. *Nat. Commun.* **2015**, *6*, 6337.

14. Faller, M.; Niederweis, M.; Schultz, G. E. The Structure of a Mycobacterial Outer Membrane Channel. *Science* **2004**, *303*, 1189–1192.

15. Sui, H.; Han, B.-G.; Lee, J. K.; Walian, P.; Jap, B. K. Structural Basis of Water-Specific Transport Through the AQP1 Water Channel. *Nature* **2001**, *414*, 872–878.